TABLE II
CAPACITANCE AND POTENTIAL COEFFICIENT MATRIX ELEMENTS FOR TWO COUPLED MICROSTRIPS OF EQUAL WIDTH AND ZERO THICKNESS ON A 105-MM-THICK SUBSTRATE (5-μm SiN, $Ec = 4.1$, ON TOP OF 100-μm InP, $Eg = 12.5$). FORMULAS (5)–(8) COMPARED TO MoL [7]

	W [μm]	d [μm]	Λ_{11}	Λ_{12}	C_{10}	C_{12}
MoL	3.75	4.5	0.1965	0.1174	3.186	4.726
Eq. (5)-(8)			0.2013	0.1080	3.233	3.741
MoL	3.75	10.5	0.2029	0.0700	3.666	1.930
Eq. (5)-(8)			0.2013	0.0708	3.674	1.994
MoL	12.5	25	0.1334	0.0430	5.668	2.695
Eq. (5)-(8)			0.1320	0.0433	5.703	2.788
MoL	12.5	40	0.1338	0.0307	6.082	1.808
Eq. (5)-(8)			0.1320	0.0308	6.143	1.867
MoL	12.5	80	0.1339	0.0156	6.693	0.880
Eq. (5)-(8)			0.1320	0.0146	6.820	0.849
MoL	37.5	138	0.0835	0.0069	11.07	0.990
Eq. (5)-(8)			0.0838	0.0061	11.13	0.872

VII. CONCLUSION AND PHYSICAL IMPLEMENTATION

We have shown that the proposed method using the simplified parameter dependence of the inverted capacitance coefficient matrix to generate capacitance values is applicable to very general configurations of parallel lines. Shielding effects from inserted lines and proximity effects on ground capacitance are taken care of automatically. The assumptions do not necessarily hold for overlapping microstrip lines, i.e., when the ground plane is shielded.

For an IC process with a semiisolating substrate, both accurate numerical and experimental determination of parametrized look-up tables is a straightforward task. Test structures with two coupled lines of standard width (W_i) and covering a range of distances (d_{ij}) could be experimentally characterized in a network analyzer at frequencies low enough to ensure pure capacitive behavior, but high enough to yield accurate results (usually 50–500 MHz).

When the bulk substrate is resistive, as with Si, things get more complicated. Inductance is calculated with line distance to ground equal to the full chip thickness as long as skin depth in the bulk is much greater than bulk thickness, i.e., for frequencies below a value proportional to bulk resistivity divided by bulk thickness squared (about 6 GHz for 1-mm-thick 10-Ω·cm Si). For most practical cases, the frequency is low enough. Capacitance consists of a series connection of an oxide layer and a lossy bulk. Below the frequency, where $\omega\varepsilon\varepsilon_0$ equals σ, the bulk capacitor tends to be short circuited. Above that frequency, the displacement current dominates the space down to ground; in between there is a lossy region. For 10-Ω·cm Si, this dividing frequency is 15 GHz, but for 1000 Ω·cm it is 150 MHz. Thus, a 10-Ω·cm Si process may safely be characterized at 50–500 MHz and yields values typical for the oxide layer. A 1000-Ω·cm Si process intended for applications at gigahertz frequencies will work with lower capacitance to ground corresponding to the full substrate thickness, and characterization should be made at 500–1000 MHz.

REFERENCES

[1] P. Feldmann and R. W. Freund, "Efficient linear circuit analysis by Padé approximation via the Lanczos process," *IEEE Trans. Computer-Aided Design*, vol. 14, pp. 639–649, May 1995.

[2] A. R. Djordjević, M. B. Bazdar, T. K. Sarkar, and R. F. Harrington, *LINPAR for Windows: Matrix Parameters for Multiconductor Transmission Lines*. Norwood, MA: Artech House, 1995.

[3] U. Choudhury and A. Sangiovanni-Vincentelli, "Automatic generation of analytical models for interconnect capacitances," *IEEE Trans. Computer-Aided Design*, vol. 14, pp. 470–480, Apr. 1995.

[4] C. S. Walker, *Capacitance, Inductance and Crosstalk Analysis*. Norwood, MA: Artech House, 1990, pp. 88–102.

[5] E. Hallén, *Elektricitetslära*. Stockholm, Sweden: Almqvist & Wiksell, 1953, pp. 50, 226–234.

[6] H. A. Wheeler, "Formulas for the skin effect," *Proc. IRE*, vol. 30, no. 9, pp. 412–424, 1942.

[7] U. Schulz and R. Pregla, "A new technique for the analysis of the dispersion characteristics of planar waveguides," *Arch. Elektron. Uebertrag. Tech.*, vol. 34, no. 4, pp. 169–173, 1980.

[8] J. Siegl, V. Tulaja, and R. Hoffmann, "General analysis of interdigitated microstrip couplers," *Siemens Forsch. Entwickl.ber.*, vol. 10, no. 4, pp. 228–236, 1981.

Comparison Between Theoretical and Measured Microstrip Gap Parameters Involving Anisotropic Substrates

Jesús Martel, Francisco Medina, Rafael R. Boix, and Manuel Horno

***Abstract*— In this paper, experimental results are presented for microstrip symmetrical-gap discontinuities. The experimental technique is based on the measurement of the resonant frequencies of several gap-coupled rectangular microstrip resonators. In particular, gap discontinuities on anisotropic dielectric and two-layer composite substrates have been investigated. Reasonably good agreement has been found in most cases between theoretical data [obtained by means of the excess charge technique in the spectral domain (EC-SDA)] and experimental data, even though the theoretical results have been obtained by using a quasi-static approach.**

***Index Terms*—Anisotropic media, microstrip discontinuities, microwave measurements.**

I. INTRODUCTION

The correct characterization of the microstrip gap effect is essential for accurately predicting the frequency response of filters based on end-to-end coupled rectangular resonators [1]. In a former paper, the authors used the excess charge technique in the spectral domain (EC-SDA) in order to obtain numerical results for the equivalent circuit parameters of some microstrip gap discontinuities [2]. This technique is electrostatic in nature, but it has been reported that the equivalent-circuit parameters of microstrip gap discontinuities show a very slight variation with frequency [3]. In this paper, the quasi-static results obtained with the technique presented in [2] are compared with measured results. In particular, emphasis is placed on testing gap discontinuities printed on anisotropic substrates and composite two-layer substrates.

In this paper, a resonance technique is used for measuring the equivalent lengths of symmetric microstrip gaps. This type of experimental setup has been traditionally employed in the literature for characterizing microstrip discontinuities [3]–[8]. The technique is based on the measurement of the resonant frequencies of resonant

Manuscript received December 9, 1996; revised November 21, 1997. This paper was supported by the DGICYT, Spain, under Project TIC95-0447.

The authors are with the Grupo de Microondas (Departamento de Electrónica y Electromagnetismo), Universidad de Sevilla, 41012 Sevilla, Spain.

Publisher Item Identifier S 0018-9480(98)01599-3.

circuits in which the discontinuities under test are embedded. One advantage of our experimental procedure is that it makes it possible to remove some of the error sources related to uncertainties in physical dimensions. This is achieved by using the same physical circuit for the two resonant systems involved in the measurement of the gaps' equivalent lengths.

II. Experimental Setup and Procedure

The experimental technique we have employed is a modified version of the resonance method proposed by Gupta *et al.* in [5]. The basic resonant structure is shown in Fig. 1(a). It consists of two straight rectangular resonators coupled through the symmetric gap to be measured. These two resonators are fed by two 50-Ω microstrip lines coupled through two identical asymmetric gaps. The 50-Ω lines are connected to the coaxial ports of an HP-8510-B ANA. The equivalent circuit associated to the structure in Fig. 1(a) is shown in Fig. 1(b).

The circuit in Fig. 1(b) will present both even and odd resonances. In the even (odd) resonances, the symmetry plane AA' [Fig. 1(a)] behaves as a magnetic (electric) wall. Let l be the actual physical length of the resonators. Let $\Delta l_f^{e(n)}$ ($\Delta l_f^{o(n)}$) be the equivalent length of the feeding gap and $\Delta l_g^{e(n)}$ ($\Delta l_g^{o(n)}$) the equivalent length of the symmetric gap to be measured at the nth even (odd) resonant frequency $f_e^{(n)}$ ($f_o^{(n)}$). Thus, the total equivalent length of each resonator at that frequency $l_t^{e(n)}$ ($l_t^{o(n)}$) is

$$l_t^{i(n)} = \Delta l_f^{i(n)} + l + \Delta l_g^{i(n)} = \frac{nc}{2\sqrt{\varepsilon_{\rm ef}^{i(n)}} f_i^{(n)}}, \qquad i = e, o \tag{1}$$

where c is the speed of light in vacuum and $\varepsilon_{\rm ef}^{e(n)}$ ($\varepsilon_{\rm ef}^{o(n)}$) is the effective dielectric constant of the resonant transmision-line sections of Fig. 1(b) at the frequency $f_e^{(n)}$ ($f_o^{(n)}$). Since dispersion for microstrip lines is weak, the small difference between $f_e^{(n)}$ and $f_o^{(n)}$ makes it possible to assume that $\varepsilon_{\rm ef}^{e(n)} = \varepsilon_{\rm ef}^{o(n)} = \varepsilon_{\rm ef}^{(n)}$. In addition, since the field configuration around the feeding gaps is almost the same in both nth even and odd resonances, we can also assume that $\Delta l_f^{e(n)} = \Delta l_f^{o(n)} = \Delta l_f^{(n)}$.

By filling the nonmetallized symmetrical-gap area in Fig. 1(a) with conducting ink, it is possible to obtain a second measurement block consisting of a single straight resonator of physical length $L = 2l + s$. Let $f_L^{(2n)}$ be the $2n$th resonant frequency of this resonator. The total equivalent length at this frequency is given by

$$l_t^{L(2n)} = 2l + s + 2\Delta l_f^{L(2n)} = \frac{nc}{\sqrt{\varepsilon_{\rm ef}^{L(2n)}} f_L^{(2n)}}. \tag{2}$$

Since the value of $l_t^{L(2n)}$ will be roughly twice the value of $l_t^{e(n)}$ or $l_t^{o(n)}$, the $2n$th resonant frequency of the new resonator $f_L^{(2n)}$ will be close to $f_e^{(n)}$ and $f_o^{(n)}$ and, therefore, we can assume that effective dielectric constant and feeding-gap equivalent length appearing in (2) coincide with those appearing in (1), i.e., $\varepsilon_{\rm ef}^{L(2n)} = \varepsilon_{\rm ef}^{(n)}$ and $\Delta l_f^{L(2n)} = \Delta l_f^{(n)}$. Bearing in mind this latter assumption from (1) and (2), we can derive the following expressions:

$$\Delta l_g^{o(n)} - \Delta l_g^{e(n)} = \frac{nc}{2\sqrt{\varepsilon_{\rm ef}^{(n)}}} \left[\frac{1}{f_o^{(n)}} - \frac{1}{f_e^{(n)}} \right] \tag{3}$$

$$\Delta l_g^{e(n)} = \frac{s}{2} + \frac{nc}{2\sqrt{\varepsilon_{\rm ef}^{(n)}}} \left[\frac{1}{f_e^{(n)}} - \frac{1}{f_L^{(2n)}} \right]. \tag{4}$$

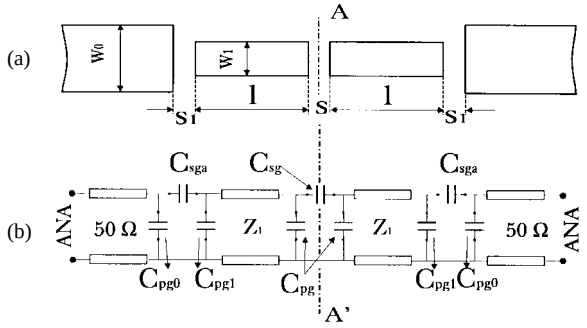

Fig. 1. (a) Basic measurement block. (b) Circuit representation of (a).

Note that (3) and (4) are a couple of equations for $\Delta l_g^{e(n)}$ and $\Delta l_g^{o(n)}$ where the errors arising from uncertainties in the measurement of l have been removed, which is because the two resonant configurations involved in the measurements have *strictly* the same value of l.

According to (3) and (4), the key step in the experimental determination of $\Delta l_g^{o(n)} - \Delta l_g^{e(n)}$ and $\Delta l_g^{e(n)}$ is the measurement of $f_e^{(n)}$, $f_o^{(n)}$, and $f_L^{(2n)}$. These frequencies can be measured to a very high precision (around 0.005% error) by using the HP-8510-B ANA. In this paper, the measurements were carried out 40 times at different moments and with different calibrations in order to account for random experimental errors [8] (see error bars in the experimental results presented in the following section). Once $f_e^{(n)}$, $f_o^{(n)}$, and $f_L^{(2n)}$ are known, the determination of $\Delta l_g^{o(n)} - \Delta l_g^{e(n)}$ and $\Delta l_g^{e(n)}$ via (3) and (4) requires the experimental evaluation of $\varepsilon_{\rm ef}^{(n)}$. In this paper, $\varepsilon_{\rm ef}^{(n)}$ was obtained by fitting our measured data for $f_e^{(n)}$, $f_o^{(n)}$, and $f_L^{(2n)}$ with numerical data extracted from the computer-simulated response of the circuit of Fig. 1(b). In order to generate these latter numerical results, the characteristic impedance of the microstrip lines of Fig. 1(a) was computed by using a full-wave spectral-domain analysis (SDA) [9] and the gap capacitances were computed by means of the quasi-static numerical technique reported in [2].

III. Experimental Results

In this section, the experimental results obtained for the equivalent lengths of several microstrip gap discontinuities are presented and compared to quasi-static results computed by the EC-SDA [2]. When the EC-SDA is applied to the analysis of microstrip gap discontinuities, the parameters that are obtained are the capacitances C_{sg} and C_{pg} of Fig. 1(b) [2]. The computation of $\Delta l_g^{o(n)} - \Delta l_g^{e(n)}$ and $\Delta l_g^{e(n)}$ in terms of C_{sg} and C_{pg} can be carried out in two different ways. The first possibility is to use quasi-static models to characterize both the gap discontinuities [2] and the microstrip lines involved in those discontinuities [10]. In this case, we simply have

$$\begin{aligned} \Delta l_g^{o(n)} - \Delta l_g^{e(n)} &= \frac{2C_{sg}}{C_1^{\infty}} \\ \Delta l_g^{e(n)} &= \frac{C_{pg}}{C_1^{\infty}} \end{aligned} \tag{5}$$

where C_1^{∞} is the capacitance per unit length of the microstrip lines [10]. Note that (5) implies that $\Delta l_g^{o(n)}$ and $\Delta l_g^{e(n)}$ are frequency independent, which is only an approximation. The second possible way to obtain $\Delta l_g^{o(n)} - \Delta l_g^{e(n)}$ and $\Delta l_g^{e(n)}$ in terms of C_{sg} and C_{pg} is to employ a hybrid model in which static-analysis EC-SDA is used to characterize the gap discontinuities, but full-wave analysis [9] is used to characterize the microstrip lines. When we use this hybrid

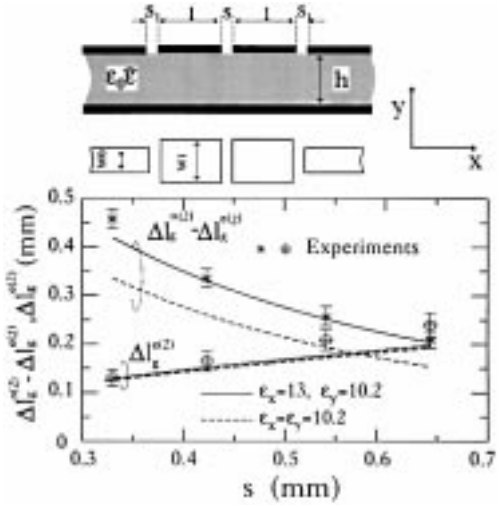

Fig. 2. Theoretical and experimental values of $\Delta l_g^{o(2)} - \Delta l_g^{e(2)}$ and $\Delta l_g^{e(2)}$ for microstrip gaps on E-10 substrate as a function of gap spacing. Theoretical values have been calculated by considering E-10 both as isotropic dielectric material (dashed lines) and as an anisotropic dielectric material (solid lines). The measured resonance frequencies are in the band 6.72–6.93 GHz. Geometry: $h = 0.635$ mm, $w_0 = 0.61$mm, $w_1 = 1.38$ mm, $l = 15$ mm, $s_1 = 0.2$ mm.

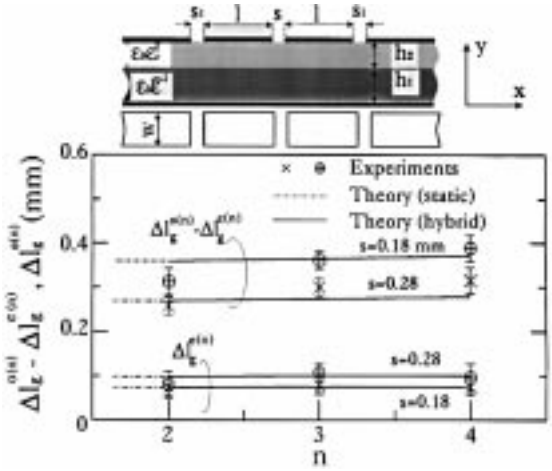

Fig. 3. Theoretical and experimental values of $\Delta l_g^{o(n)} - \Delta l_g^{e(n)}$ and $\Delta l_g^{e(n)}$ for two microstrip gaps on two-layer E-10/PTFE woven glass substrate ($\varepsilon_x^1 = 13$, $\varepsilon_y^1 = 10.2$, $\varepsilon_r^2 = 2.53$) as a function of the order of the resonance (n) and of the gap spacing (s). Geometry: $h_1 = 0.635$ mm, $h_2 = 0.135$ mm, $w = 1.23$ mm, $l = 15$ mm, $s_1 = 0.3$ mm. The resonance frequency bands are 9.12–9.55 GHz for $n = 2$, 13.3–14.2 GHz for $n = 3$, and 17.4–18.3 GHz for $n = 4$.

model in Fig. 1(a), theoretical values of $f_e^{(n)}$, $f_o^{(n)}$, and $f_L^{(2n)}$ can be computed and then introduced into (3) and (4) to obtain the theoretical values of $\Delta l_g^{o(n)} - \Delta l_g^{e(n)}$ and $\Delta l_g^{e(n)}$ that will be checked against the experimental values.

In Fig. 2 we plot theoretical (static model) and experimental values of $\Delta l_g^{o(2)} - \Delta l_g^{e(2)}$ and $\Delta l_g^{e(2)}$ for four different microstrip gap discontinuities. The discontinuities are printed on E-10 substrate. The nominal relative dielectric constant provided by manufacturer for this material is $\varepsilon_r = 10.2$. However, E-10 has been reported to present dielectric anisotropy [11]. Apparently, E-10 behaves as an uniaxial anisotropic dielectric material having different dielectric constants in the directions perpendicular ($\varepsilon_y = 10.2$) and parallel ($\varepsilon_x = 13.0$) to the metallic surfaces. We have made theoretical estimations of the equivalent lengths of the gaps analyzed in Fig. 2 by assuming that the substrate is isotropic as well as anisotropic. Both theoretical predictions have been included in the figure in order to compare with measured results. Notice that the influence of the anisotropy on the theoretical results for $\Delta l_g^{e(2)}$ seems to be very small. This fact can be easily explained if we consider that $\Delta l_g^{e(2)}$ is related to the capacitance $C_{\rm pg}$ [see (5)]. Since this capacitance mainly accounts for y-directed fringing electric fields, its value will essentially depend on ε_y, which has been taken to be the same in both the isotropic and the anisotropic models of E-10. On the contrary, there are important differences (reaching 30%) between the theoretical values of $\Delta l_g^{o(2)} - \Delta l_g^{e(2)}$ obtained when we use either the isotropic or the anisotropic model for E-10. This is because that parameter is closely related to C_{sg} [see (5)], and C_{sg} mainly accounts for the x-directed fringing electric fields of the gap discontinuities. Thus, C_{sg} is strongly influenced by ε_x, which is the dielectric constant making the difference between the isotropic and the anisotropic models of the substrate. It can be noticed that the measured values of $\Delta l_g^{o(2)} - \Delta l_g^{e(2)}$ appearing in Fig. 2 agree much better with the theoretical values of $\Delta l_g^{o(2)} - \Delta l_g^{e(2)}$ obtained when the anisotropic nature of E-10 is accounted for. This would be in accordance with the behavior of E-10 reported in [11].

Finally, Fig. 3 shows theoretical (static and hybrid model) and experimental results for the equivalent lengths of microstrip gap discontinuities printed on a double-layer substrate: the upper layer is polytetrafluorethylene (PTFE) woven glass material and the lower layer is E-10. Note that the agreement between theoretical and experimental results is good (worst cases correspond to differences ranging between 10%–15%). It should be pointed out that in the frequency range swept in Fig. 3 (roughly 9–18 GHz) the equivalent lengths of the gaps analyzed present a weak frequency dependence and, therefore, theoretical static and hybrid predictions do not differ much.

IV. Conclusion

In this paper, the authors have presented an experimental technique for the measurement of the equivalent lengths of microstrip symmetrical-gap discontinuities. The experimental technique is based on the measurement of the resonant frequencies of two microstrip resonator configurations, and it is designed in such a way that it makes it possible to remove inaccuracies due to uncertainties in the measurement of the resonator lengths. Measurements of microstrip gaps on anisotropic and double-layered substrates have been carried out. The experimental results have been compared with theoretical predictions based on EC-SDA, and agreement has been found to be satisfactory. In particular, it has been shown that the effect of substrate dielectric anisotropy should not be neglected in characterizing microstrip gap discontinuities.

References

[1] R. K. Hoffmann, *Handbook of Microwave Integrated Circuits*. Norwood, MA: Artech House, 1987.

[2] J. Martel, R. R. Boix, and M. Horno, "Static analysis of microstrip discontinuities using the excess charge technique in the spectral domain," *IEEE Trans. Microwave Theory Tech.*, vol. 39, pp. 1623–1631, Sept. 1991.

[3] V. Rizzoli and A. Lipparini, "A resonance method for the broad-band characterization of general two-port microstrip discontinuities," *IEEE Trans. Microwave Theory Tech.*, vol. MTT-29, pp. 655–660, July 1981.

[4] B. Easter, "The equivalent circuits of some microstrip discontinuities," *IEEE Trans. Microwave Theory Tech.*, vol. MTT-23, pp. 655–661, Aug. 1975.

[5] C. Gupta, B. Easter, and A. Gopinath, "Some results on the end effects of microstrip lines," *IEEE Trans. Microwave Theory Tech.*, vol. MTT-26, pp. 649–652, Sept. 1978.

[6] M. Kirschning, R. H. Jansen, and N. H. L. Koster, "Measurement and computer-aid modeling of microstrip discontinuities by an improved resonator method," in *IEEE MTT-S Int. Microwave Symp. Dig.*, Boston, MA, June 1983, pp. 495–497.

[7] A. J. Slobodnik, R. T. Webster, and G. A. Roberts, "18–42 GHz experimental verification of microstrip coupler and open end capacitance models," *IEEE Trans. Microwave Theory Tech.*, vol. 40, pp. 584–587, Mar. 1992.

[8] A. J. Slobodnik and R. T. Webster, "Experimental validation of microstrip bend discontinuity models from 18 to 60 GHz," *IEEE Trans. Microwave Theory Tech.*, vol. 42, pp. 1872–1877, Oct. 1994.

[9] G. Cano, F. Medina, and M. Horno, "Efficient spectral domain analysis of generalized multistrip lines in stratified media including thin, anisotropic, and lossy substrate," *IEEE Trans. Microwave Theory Tech.*, vol. 40, pp. 217–227, Feb. 1992.

[10] F. Medina and M. Horno, "Quasi-analytical static solution of the boxed microstrip line embedded in a layered medium," *IEEE Trans. Microwave Theory Tech.*, vol. 40, pp. 1748–1756, Sept. 1992.

[11] N. G. Alexopoulos, "Integrated-circuits structures on anisotropic substrates," *IEEE Trans. Microwave Theory Tech.*, vol. MTT-33, pp. 847–881, Oct. 1985.